



HAL
open science

Oscillations and decay of superfluid currents in a one-dimensional Bose gas on a ring

Juan Polo, Romain Dubessy, Paolo Pedri, H el ene Perrin, Anna Minguzzi

► **To cite this version:**

Juan Polo, Romain Dubessy, Paolo Pedri, H el ene Perrin, Anna Minguzzi. Oscillations and decay of superfluid currents in a one-dimensional Bose gas on a ring. *Physical Review Letters*, 2019, 123, pp.195301. 10.1103/PhysRevLett.123.195301 . hal-02078189

HAL Id: hal-02078189

<https://hal.science/hal-02078189>

Submitted on 25 Mar 2019

HAL is a multi-disciplinary open access archive for the deposit and dissemination of scientific research documents, whether they are published or not. The documents may come from teaching and research institutions in France or abroad, or from public or private research centers.

L'archive ouverte pluridisciplinaire **HAL**, est destin ee au d ep ot et  a la diffusion de documents scientifiques de niveau recherche, publi es ou non,  emanant des  tablissements d'enseignement et de recherche fran ais ou  trangers, des laboratoires publics ou priv es.

Oscillations and decay of superfluid currents in a one-dimensional Bose gas on a ring

Juan Polo,¹ Romain Dubessy,² Paolo Pedri,² H el ene Perrin,² and Anna Minguzzi¹

¹Univ. Grenoble Alpes, CNRS, LPMMC, 38000 Grenoble, France

²Laboratoire de physique des lasers, CNRS, Universit e Paris 13, Sorbonne Paris Cit e, 99 avenue J.-B. Cl ement, F-93430 Villetaneuse, France

(Dated: March 25, 2019)

We study the time evolution of a supercurrent imprinted on a one-dimensional ring of interacting bosons in the presence of a defect created by a localized barrier. Depending on interaction strength and temperature, we identify various dynamical regimes where the current oscillates, is self-trapped or decays with time. We show that the dynamics is captured by a dual Josephson model, and involves phase slips of thermal or quantum nature.

Superfluidity is a fascinating phenomenon emerging in interacting quantum systems and governing their low temperature transport properties. Supercurrents, named in analogy with superconductivity, are characterized, among others, by frictionless flow and quantized vortices, and are most easily evidenced in ring geometries. Ultra-cold atoms confined in ring traps have proven to be a great tool to study superfluid transport properties [1–3]. Due to their tunability and their high degree of control, they are an ideal system for studying the effect of interactions and dimensionality in the superfluid transport dynamics. As superconducting SQUIDs have provided a wealth of applications, the realization of their atomic analogs – the AQUID [4] – is a first step in the whole new field of atomtronics [5, 6].

From a fundamental point of view, an open question is the stability of supercurrents. For a three-dimensional (3D) ring geometry the stochastic decay of the quantized current has been studied, evidencing the role of the critical velocity [2, 7]. In the presence of a repulsive barrier crossing the ring, resulting in a weak link, hysteresis in the phase slips dynamics has been investigated [8–11] and the role of thermal activation evidenced [12]. A scenario for the phase slips dynamics induced by a weak link based on the role of vortices can be used to explain qualitatively the experimental observations [13] but fails to account quantitatively for the thermal activation [14, 15].

In this context one question naturally arises: if the phase slips dynamics is driven in 3D by vortices crossing the weak link, what happens in lower dimension? While in two-dimensional (2D) systems vortices still play a crucial role in the superfluid dynamics [4, 13], they cannot exist in one-dimension (1D). Therefore the phase slips phenomenon should be of a different nature in 1D.

Previous works have shown the role of phase-slips [16] in the decay of 1D transport in the presence of periodic perturbation [17]. For a microscopic impurity the decay rate has been estimated by computing the drag force [18]. For sufficiently small obstacles stationary circulating states may exist [19, 20], while a forced flow past a larger obstacle results in soliton emission [21, 22]. Most of these previous studies were performed in a rotat-

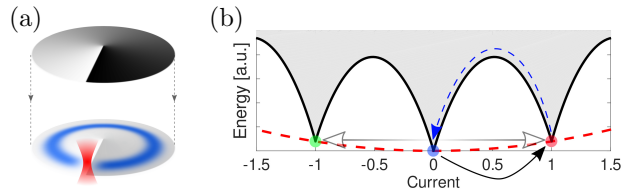


FIG. 1. (a) Sketch of the quench protocol: a 1D Bose gas is trapped in a ring, in the presence of a localized barrier, e.g. a tightly focused repulsive optical potential (red), creating a dip in the density (blue), and quenched out of equilibrium by imprinting a phase gradient. (b) Energy landscape of the homogeneous 1D Bose gas on a ring: the states with integer values of the current per particle correspond to local minima of the energy. The quench (black arrow) transfers the system from the initial zero-current state (light blue circle) to the state with one unit of current (light red circle). Depending on the parameters, the barrier will then resonantly couple the +1 and -1 states (light gray arrow) or induce an adiabatic transition between the +1 and 0 states (dashed blue arrow), see text for details.

ing frame, thus *imposing* a flow onto the ring, allowing to estimate the nucleation rate of phase-slips [23]. For intermediate to strong interactions and small impurities it has been shown that the nature of the decay of persistent currents is related to the low-energy phonon excitations within the ring [24].

In this work, we investigate how a *free* current flows in 1D: as illustrated in Fig. 1, starting from a system initially prepared in a well-defined current state in a ring trap with a barrier, we follow its dynamics with the aim of elucidating the current dynamics and its dissipation mechanisms. Our study concerns both zero- and finite temperature gases, both at weak and strong interactions. We show that the dynamical behavior can be interpreted as a dual of the Josephson effect, occurring among angular momentum states. Depending on the barrier strength and the temperature regime we observe current oscillations, self-trapping or decay. In the weakly interacting regime, we show that the observed dynamics corresponds to self trapping among angular momentum states at zero temperature, and that the decay of the currents at fi-

nite temperature involves dark solitons. For strong interactions, we show that coherent quantum phase slips dominate the current dynamics at zero temperature, and incoherent ones take over at finite temperature.

Model We study an ensemble of N bosons of mass m with repulsive contact interactions on a ring of circumference L with periodic boundary conditions, i.e. the Lieb-Liniger model, generalized to include the presence of an external barrier potential $V(x)$. The Hamiltonian reads:

$$\hat{\mathcal{H}} = \int_0^L dx \hat{\Psi}^\dagger \left(-\frac{\hbar^2}{2m} \frac{\partial^2}{\partial x^2} + V(x) + \frac{g}{2} \hat{\Psi}^\dagger \hat{\Psi} \right) \hat{\Psi}, \quad (1)$$

where $\hat{\Psi}$ is the bosonic field operator and the corresponding average density is $n = N/L$ with the total number of particles given by $\int_0^L dx \langle \hat{\Psi}^\dagger \hat{\Psi} \rangle = N$. This model describes e.g. ultra-cold atoms confined in a tight ring trap. In this case $g = 2\hbar\omega_\perp a_s$ is the one-dimensional interaction strength, ω_\perp the radial confinement frequency and a_s the 3D s -wave scattering length. In the following we will consider either a delta potential $V(x) = \alpha\delta(x)$, for which analytical results can be obtained, or a Gaussian potential $V(x) = V_0 \exp\left(-\frac{x^2}{2\sigma^2}\right)$, realistic from the experimental point of view. For homogeneous 1D gases the equilibrium properties at finite temperature are captured by two dimensionless parameters [26]: $\gamma = \frac{mg}{\hbar^2 n}$ quantifying the interaction regime from weakly ($\gamma \ll 1$) to strongly interacting ($\gamma \gg 1$), and the reduced temperature $\tau = \frac{T}{T_d \gamma^2}$, where $T_d = \hbar^2 n^2 / 2mk_B$ is the quantum degeneracy temperature.

Quench protocol Our goal is to study the dynamics of the particle current in the presence of a barrier. We first prepare the system in an equilibrium state Ψ_0 in the presence of the static barrier potential. This results in a state with no current. Specific details on the implementation depend on the interaction regime and are given later. We then quench the current by phase imprinting a specific circulation onto the many-body wavefunction: $\Psi_0(x_1, \dots, x_N) \rightarrow \Psi_1(x_1, \dots, x_N) = \Psi_0 \times e^{i2\pi\ell \sum_j x_j / L}$. Note that this process can be implemented in experiments using specific light potentials according to various available schemes [2, 27]. We then monitor the current by computing the average of the current operator:

$$J(t) = -i \frac{\hbar}{2m} \frac{1}{N} \int_0^L \frac{dx}{L} \left\langle \hat{\Psi}^\dagger \partial_x \hat{\Psi} - \partial_x \hat{\Psi}^\dagger \hat{\Psi} \right\rangle. \quad (2)$$

The subsequent time evolution after the quench is described by the following approaches depending on the interaction and temperature regimes: (i) at $T = 0$ and for a weakly interacting gas ($\gamma \ll 1$) we rely on the Gross-Pitaevskii equation (GPE) numerical solution and on an analytical two-mode model adapted from [28]; (ii) at $T > 0$ and $\gamma \ll 1$ we use the Projected Gross-Pitaevskii equation (PGPE) formalism [29, 30] and (iii)

at $\gamma \gg 1$ we rely on the exact time-dependent Bose-Fermi mapping describing the infinitely strong interaction Tonks-Girardeau (TG) limit for the whole temperature range [31–33]. In this work we focus on a quench with circulation $\ell = 1$.

In the weakly interacting limit it is natural to define the barrier strength relative to the chemical potential, i.e., we define a Gaussian barrier strength as $\lambda_{GP} = V_0/\mu_0$ with $\mu_0 = gn$ being the chemical potential of the homogeneous annular gas. Figure 2 illustrates the results of our simulations in the weakly interacting regime as a function of this barrier strength, for a relatively narrow barrier of width $\sigma = L/50$, yet much larger than the healing length $\xi = \hbar/\sqrt{2mgn}$.

At zero temperature we observe in Fig. 2(a) that the current remains very close to the initial quenched circulating state for weak to moderate barriers, up to $\lambda_{GP} \sim 1$. Above this critical value, we observe a fast decay of the current, followed by oscillations around the 0 value. This is very similar to what has been obtained in 2D simulations [14]. The new feature of the 1D mean-field regime is the emergence of current oscillations at large barriers. As we discuss here below, this behavior can be interpreted as the transition from self-trapping to Josephson oscillations of the currents, in analogy to the well known Josephson effect for particle imbalance predicted in [28] and experimentally observed using ultra-cold atoms confined in a double well trap [34]. In essence (see Supplemental Material for details), we derive a fully analytical two-mode model for two current states and demonstrate that this accurately captures the Gross-Pitaevskii dynamics at zero temperature and very weak interactions (see the inset of Fig. 2(a)). This model predicts a transition from self-trapping to Josephson oscillations for a critical value λ_{GP}^c that depends on the strength of interactions, as in [28]. Although the two-mode model breaks down for large barrier or higher (but still weak) interactions due to the spread of the mean-field wavefunction onto many single particle orbitals, we observe the same qualitative behavior in the simulations. Indeed, surprisingly, the current always oscillates regularly at large barriers, with a triangular shape and very small damping rate. These oscillations can be understood using a hydrodynamic description with a transport mediated by shock waves, thus at constant velocity, within an almost hard-wall container [21].

For temperature $T = \mu_0/k_B$, corresponding to the quasi-condensate regime [26], the dynamics of the current is quite different from the zero-temperature case, see Fig. 2(b). At low barriers, i.e. $\lambda_{GP} \leq 0.5$, we observe an exponential decay of the current with a decay rate increasing with the barrier strength. For larger barriers we observe damped cosine oscillations of the current. In this regime thermal phase slips occur at the position of the barrier where the density vanishes. The transition from exponential to damped oscillation decay is quali-

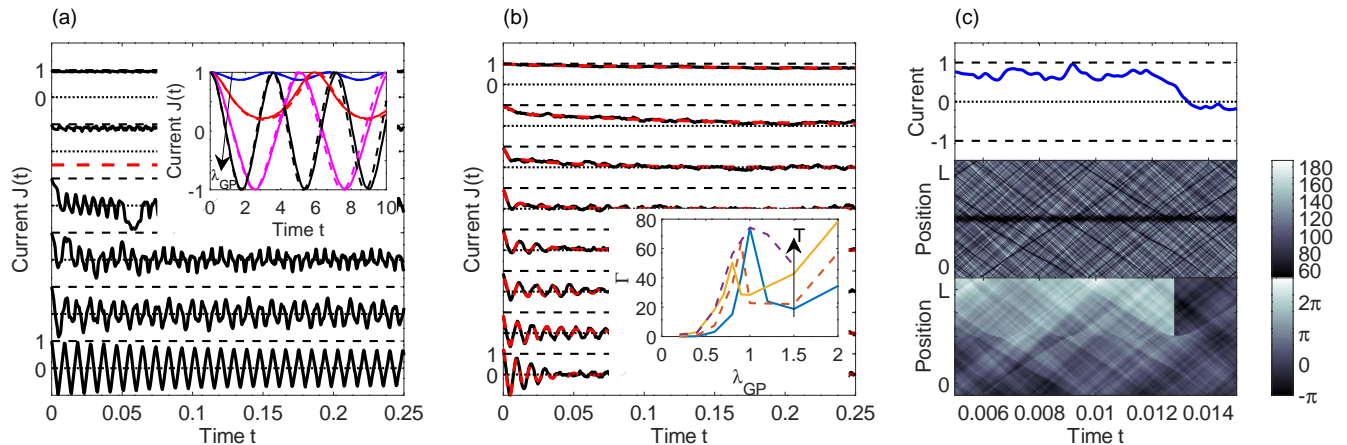


FIG. 2. (color online) Average current per particle as a function of time (in units of mL^2/\hbar) after the quench in the mean field regime for $g = 20 \times \hbar^2/(mL)$ and $N = 1000$ (so that $\gamma = 0.02$). On all graphs the black dotted (dashed) lines are horizontal guides to the eye for the current values $0 (\pm 1)$. (a) Expectation value of the current at $T = 0$ (solid lines) for different barrier strength $\lambda_{GP} = \{0.8, 1, 1.05, 1.1, 1.2, 2\}$, from top to bottom. An offset has been added to each curve for clarity. The red dashed line indicates the separation between the self-trapped and decaying regimes, see text for details. The inset displays the current evolution after a quench for a much smaller $\gamma = 2 \times 10^{-5}$, showing the agreement between the simulations (solid lines) and the two-mode model (dashed lines) for $\lambda_{GP} = \{0.05, 0.1, 0.15, 0.2\}$ (from top to bottom, following the arrow). (b) Expectation value of the current at $T = \mu_0/k_B$ (solid lines), averaged over 100 realizations of the classical field, for different barrier strength $\lambda_{GP} = \{0.4, 0.6, 0.7, 0.8, 0.9, 1, 1.5, 2\}$, from top to bottom. The overlaid red dashed curves are the results of fits allowing to extract the typical damping rate of the current. The inset displays the decay rates Γ obtained from the fit [25], for temperatures $T = \{0.5, 1, 1.5, 1.75\} \times \mu_0/k_B$ (from bottom to top, following the arrow), see text for details. (c) Zoom on a single classical field trajectory, for $T = \mu_0/k_B$ and $\lambda = 0.6$, illustrating the phase slip phenomenon: a jump in the value of the current (top panel) is associated to the reflection of a slow soliton at the barrier visible in the density map (middle panel) and a singularity in the phase profile (bottom panel).

tatively observed for all our temperatures in the range $0.5 \leq k_B T/\mu_0 \leq 2.5$. The inset of Fig. 2(b) displays the value of the damping rate Γ given by the fit [25] for increasing temperatures, in the range $0.5\mu_0 \leq k_B T \leq 1.75\mu_0$. The damping rate increases with temperature, displaying a non-monotonous dependence on the barrier strength, with a maximum at the crossover between the two decay regimes. The crossover occurs at lower barrier strength for larger temperatures, consistent with the thermal activation of solitons.

In order to elucidate the mechanisms for the current decay, Fig. 2(c) shows a *single* classical field trajectory, showing many spontaneous thermal gray solitons [35]. While most of the solitons present a small density dip, hence are fast and are transmitted through the barrier [36], we notice that the current undergoes discrete jumps each time a soliton is reflected on the barrier: in this case, when the soliton reaches zero velocity the density profile vanishes, allowing for a phase slip to occur. This corresponds to the adiabatic process indicated by the dashed blue line on Fig. 1(b). As the temperature increases, the probability to find slow solitons increases and the jumps occur more and more frequently, resulting in an increase of the decay rate. Finally, as the barrier couples the soliton dynamics to the long wavelength sound excitations [36] we expect this process to be intrin-

sically stochastic, thus resulting in an exponential decay of the average current as observed.

The description of current dynamics as dual of the Josephson effect persists at strong interactions. In this regime, the classical picture does not apply, rather, we will show below that the dynamics corresponds to quantum coherent oscillations among angular momentum states (see [37] for the analog phenomenon in superconductors). We provide a microscopic description of the dynamics of the current in the strongly interacting limit $\gamma \gg 1$ using the exact Tonks-Girardeau solution, which maps the interacting bosons onto a Fermi gas. In the TG regime the relevant dimensionless barrier strength is $\lambda_{TG} = V_b/E_F$, with $V_b = \alpha n$ being the barrier associated energy and $E_F = \hbar^2 n^2 \pi^2 / 2m$ being the Fermi energy, corresponding to the zero-temperature chemical potential for systems displaying fermionization (see Supplemental Material). At zero temperature, Fig. 3(a), we note that for weak barriers, $\lambda_{TG} \ll 1$, in contrast to the weakly interacting regime, there is no self-trapping, rather, the current undergoes Rabi-like oscillations. These oscillations correspond to coherent quantum phase slips due to backscattering induced by the presence of the barrier. Microscopically, it corresponds to dynamical processes involving the whole Fermi sphere, i.e. multiple-particle hole excitations where each particle

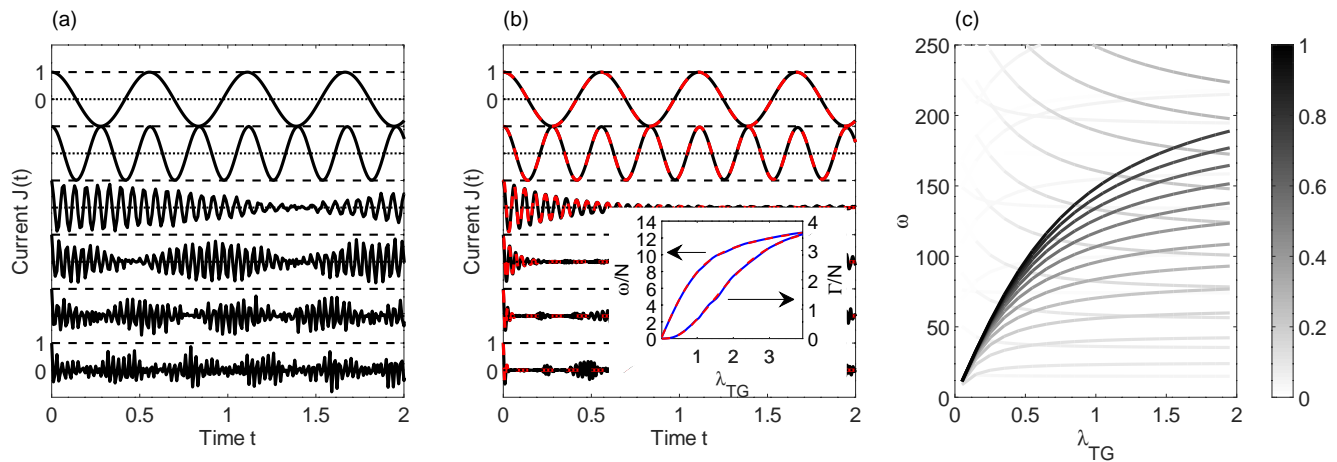


FIG. 3. (color online) Average current per particle as a function of time (in units of \hbar/mL^2) after the quench in the Tonks-Girardeau regime for $N = 23$ bosons. On all graphs the black dotted (dashed) lines are horizontal guides to the eye for the current values $0 (\pm 1)$. (a) Expectation value of the current at $T = 0$ (solid lines) for different barrier strength $\lambda_{TG} = \{0.05, 0.1, 0.5, 1, 2, 4\}$, from top to bottom. An offset has been added to each curve for clarity. (b) Expectation value of the current at $T = E_F/k_B$ (solid lines) for different barrier strength $\lambda_{TG} = \{0.05, 0.1, 0.5, 1, 2, 4\}$, from top to bottom. The overlaid red dashed curves are the results of fits allowing to extract the typical damping rate of the current. The inset shows the decay rate and frequency obtained from the fit [25], ω/N and Γ/N , as a function of λ , for $N = 11$ (solid blue curves) and $N = 23$ (dashed red curves). The two datasets fall on the same curves. (c) Frequency of the different excitations produced by the quench as a function of λ for $N = 23$ at $T = 0$. The colormap indicates the relative amplitude of the excitations.

coherently undergoes oscillations of angular momentum from $L_z = \hbar$ to $L_z = -\hbar$. As the strength of the barrier increases, an envelope appears on top of the current oscillations, degrading the Rabi oscillations. This envelope originates from the population of higher-energy modes, each transition being characterized by a different frequency, leading to a mode-mode coupling and dephasing. In Fig. 3(c) we show the frequencies and amplitudes of the various modes involved in the dynamics as a function of the barrier strength (see Supplemental Material for more details).

At finite temperatures the quench dynamics of the current involves also high-energy excitations with amplitude weighted by the Fermi distribution (see Supplemental Material for details). The resulting dynamics corresponds to an effective damping of the current oscillations with an exponential decay, see Fig. 3(b), corresponding to the effect of incoherent phase slips. The revivals observed for large barrier at zero temperature are highly suppressed due to the thermal excitations in the system. In the inset of Fig. 3(b) we show the decay rate Γ of the persistent currents as a function of the barrier strength [25]. We find that the decay of persistent currents grows monotonically with the barrier strength, since more and more excitations are involved in the dynamics as the barrier strength increases. In the same inset we show the frequency of the maximally occupied state as a function of λ_{TG} and observe that at increasing barrier strength the frequency of oscillations crosses over from a Rabi-like regime with $\omega \propto \lambda_{TG}$ to a Josephson-like regime with $\omega \propto \sqrt{\lambda_{TG}}$, in agreement with the predictions of the

low-energy Luttinger liquid theory [24]. Quite generally, while our results have been derived for infinite interaction strength, the predictions of the TG model are expected to closely describe a Bose gas at strong interactions.

In conclusion, we have shown that the dynamical evolution following a phase imprinting induces oscillations of the current in a 1D ring, associated to a rich excitation pattern, which can be described by a dual Josephson dynamics. At weak interactions and finite temperature we observe the formation of both sound waves and of thermally activated dark solitons. We find that phase-slippage occurs incoherently when the solitons are reflected by the barrier. In the strongly interacting regime at zero temperature we find coherent Rabi oscillations indicating quantum coherent phase slips, which are degraded by mode dephasing at large barrier strength or by thermal fluctuations at finite temperature. In the weakly-interacting limit we find self-trapping of current states, while no self-trapping is found at infinitely strong interactions, where quantum fluctuations dominate.

The dual Josephson picture is a new paradigm for dynamics of atomtronics circuits in which a current state encodes quantum information. Our work evidences the importance of the dynamics of the current in a 1D system, which can be accurately measured using existing experimental tools: either by using an interferometric measurement giving access to the local currents [38, 39] or by studying appropriate long wavelength excitations [40, 41]. The stochastic decay of the current in 1D via phase slips is very reminiscent of the stochastic decay due to vortex/anti-vortex recombination in 2D or

3D systems [13], where however oscillations are strongly damped by vortex creation [14]. As main difference between 1D and the higher-dimensional counterparts is that in the former case the current dynamics is more robust: at weak interactions, the solitons properties are gradually degraded by the several interactions with the barrier, mainly by sound wave radiation [36], and at strong interactions we observe the coherent dynamics of all particles. In outlook, it would be very interesting to investigate how the self-trapping disappears for large but finite interactions as well as to study the crossover to a quasi-1D geometry to explore the role of radial modes in the decay dynamics.

We thank Maxim Olshanii and Jook Walraven for stimulating discussions. We acknowledge financial support from the ANR project SuperRing (Grant No. ANR-15-CE30-0012).

-
- [1] A. Ramanathan, K. C. Wright, S. R. Muniz, M. Zelan, W. T. Hill, C. J. Lobb, K. Helmerson, W. D. Phillips, and G. K. Campbell, *Phys. Rev. Lett.* **106**, 130401 (2011).
- [2] S. Moulder, S. Beattie, R. P. Smith, N. Tammuz, and Z. Hadzibabic, *Phys. Rev. A* **86**, 013629 (2012).
- [3] D. Husmann, S. Uchino, S. Krinner, M. Lebrat, T. Giamarchi, T. Esslinger, and J.-P. Brantut, *Science* **350**, 1498 (2015).
- [4] A. C. Mathey and L. Mathey, *New Journal of Physics* **18**, 055016 (2016).
- [5] B. T. Seaman, M. Krämer, D. Z. Anderson, and M. J. Holland, *Phys. Rev. A* **75**, 023615 (2007).
- [6] L. Amico, G. Birkel, M. Boshier, and L.-C. Kwek, *New Journal of Physics* **19**, 020201 (2017).
- [7] R. Dubessy, T. Liennard, P. Pedri, and H. Perrin, *Phys. Rev. A* **86**, 011602 (2012).
- [8] K. C. Wright, R. B. Blakestad, C. J. Lobb, W. D. Phillips, and G. K. Campbell, *Phys. Rev. A* **88**, 1 (2013).
- [9] K. C. Wright, R. B. Blakestad, C. J. Lobb, W. D. Phillips, and G. K. Campbell, *Phys. Rev. Lett.* **110**, 1 (2013).
- [10] S. Eckel, J. G. Lee, F. Jendrzejewski, N. Murray, C. W. Clark, C. J. Lobb, W. D. Phillips, M. Edwards, and G. K. Campbell, *Nature* **506**, 200 (2014).
- [11] A. I. Yakimenko, K. O. Isaieva, S. I. Vilchinskii, and E. A. Ostrovskaya, *Phys. Rev. A* **91**, 023607 (2015).
- [12] A. Kumar, S. Eckel, F. Jendrzejewski, and G. K. Campbell, *Phys. Rev. A* **95**, 021602 (2017).
- [13] F. Piazza, L. A. Collins, and A. Smerzi, *Phys. Rev. A* **80**, 021601 (2009).
- [14] A. C. Mathey, C. W. Clark, and L. Mathey, *Phys. Rev. A* **90**, 023604 (2014).
- [15] M. Kunimi and I. Danshita, *Phys. Rev. A* **95**, 033637 (2017).
- [16] I. Danshita and A. Polkovnikov, *Phys. Rev. A* **85**, 1 (2012).
- [17] L. Tanzi, S. Scaffidi Abbate, F. Cataldini, L. Gori, E. Lucioni, M. Inguscio, G. Modugno, and C. D'Errico, *Scientific Reports* **6**, 25965 (2016).
- [18] A. Y. Cherny, J. S. Caux, and J. Brand, *Phys. Rev. A* **80**, 1 (2009).
- [19] L. D. Carr, C. W. Clark, and W. P. Reinhardt, *Phys. Rev. A* **62**, 063610 (2000).
- [20] M. Cominotti, D. Rossini, M. Rizzi, F. Hekking, and A. Minguzzi, *Phys. Rev. Lett.* **113**, 025301 (2014).
- [21] V. Hakim, *Phys. Rev. E* **55**, 2835 (1997).
- [22] J. A. Freire, D. P. Arovas, and H. Levine, *Phys. Rev. Lett.* **79**, 5054 (1997).
- [23] S. Khlebnikov, *Phys. Rev. A* **71**, 013602 (2005).
- [24] J. Polo, V. Ahufinger, F. W. J. Hekking, and A. Minguzzi, *Phys. Rev. Lett.* **121**, 090404 (2018).
- [25] We fit all the data sets with the same model: $J(t) = Ae^{-\Gamma_A t} + B \cos[\omega t + \phi]e^{-\Gamma_B t}$.
- [26] K. V. Kheruntsyan, D. M. Gangardt, P. D. Drummond, and G. V. Shlyapnikov, *Phys. Rev. Lett.* **91**, 040403 (2003).
- [27] A. Kumar, R. Dubessy, T. Badr, C. De Rossi, M. de Goër de Herve, L. Longchambon, and H. Perrin, *Phys. Rev. A* **97**, 043615 (2018).
- [28] A. Smerzi, S. Fantoni, S. Giovanazzi, and S. R. Shenoy, *Phys. Rev. Lett.* **79**, 4950 (1997).
- [29] M. J. Davis, S. A. Morgan, and K. Burnett, *Phys. Rev. Lett.* **87**, 1 (2001).
- [30] N. G. Berloff, M. Brachet, and N. P. Proukakis, *Proceedings of the National Academy of Sciences* **111**, 4675 (2014).
- [31] M. Girardeau, *J. Math. Phys.* **1**, 516 (1960).
- [32] M. D. Girardeau and E. M. Wright, *Phys. Rev. Lett.* **84**, 5691 (2000).
- [33] V. I. Yukalov and M. D. Girardeau, *Laser Physics Letters* **2**, 375 (2005).
- [34] M. Albiez, R. Gati, J. Fölling, S. Hunsmann, M. Cristiani, and M. K. Oberthaler, *Phys. Rev. Lett.* **95**, 010402 (2005).
- [35] T. Karpiuk, P. Deuar, P. Bienias, E. Witkowska, K. Pawłowski, M. Gajda, K. Rzążewski, and M. Brewczyk, *Phys. Rev. Lett.* **109**, 205302 (2012).
- [36] N. Bilas and N. Pavloff, *Phys. Rev. A* **72**, 033618 (2005).
- [37] O. V. Astafiev, L. B. Ioffe, S. Kafanov, Y. A. Pashkin, K. Y. Arutyunov, D. Shahar, O. Cohen, and J. S. Tsai, *Nature* **484**, 355 (2012).
- [38] L. Corman, L. Chomaz, T. Bienaimé, R. Desbuquois, C. Weintenberg, S. Nascimbene, J. Dalibard, and J. Beugnon, *Phys. Rev. Lett.* **113**, 1 (2014).
- [39] S. Eckel, F. Jendrzejewski, A. Kumar, C. J. Lobb, and G. K. Campbell, *Phys. Rev. X* **4**, 1 (2014).
- [40] G. E. Marti, R. Olf, and D. M. Stamper-Kurn, *Phys. Rev. A* **91**, 013602 (2015).
- [41] A. Kumar, N. Anderson, W. D. Phillips, S. Eckel, G. K. Campbell, and S. Stringari, *New Journal of Physics* **18**, 25001 (2016).
- [42] M. Brachet, *Comptes Rendus Physique* **13**, 954 (2012).
- [43] C. W. Gardiner, J. R. Anglin, and T. I. A. Fudge, *J. Phys. B* **35**, 1555 (2002).
- [44] C. W. Gardiner and M. J. Davis, *J. Phys. B* **36**, 4731 (2003).
- [45] G. Krstulovic and M. Brachet, *Phys. Rev. E* **83**, 066311 (2011).
- [46] K. Millard, *J. Math. Phys.* **10**, 7 (1969).
- [47] K. K. Das, M. D. Girardeau, and E. M. Wright, *Phys. Rev. Lett.* **89**, 170404 (2002).
- [48] D. Ananikian and T. Bergeman, *Phys. Rev. A* **73**, 013604 (2006).

SUPPLEMENTAL MATERIAL

Methods

Gross-Pitaevskii equation Weakly interacting bosons, with $\gamma \ll 1$, can be described at zero temperature by the well known Gross-Pitaevskii equation, obtained by considering the mean-field limit of Eq. (1):

$$i\hbar \frac{\partial \psi}{\partial t} = \left(-\frac{\hbar^2}{2m} \frac{\partial^2}{\partial x^2} + V(x) + g|\psi|^2 \right) \psi.$$

Two-mode model Within the mean field approach at zero temperature, we model the dynamics of the system after the quench by focusing on a subspace of the occupied spatial modes $\varphi_j(x)$. In particular, for weak barrier strengths, for which the Bose gas occupies mostly two modes, we use a two-mode approximation in which the wavefunction can be written as $\psi(x, t) = \phi_1(t)\varphi_1(x) + \phi_2(t)\varphi_2(x)$ [28]. The amplitudes $\phi_i(t)$ of each of these two modes correspond to the occupation of the corresponding angular momentum states, while $\varphi_{1(2)}(x)$, which are built as a symmetric (antisymmetric) combination of the first and second excited states, produce states with $\pm\ell$ angular momentum. Note however that, at difference from Ref.[28], both modes $\varphi_j(x)$ coexist in space and their orthogonality is given by their relative phase and not by their physical spatial separation.

This simplified model allows us to describe the dynamics of the current in terms of the Josephson equations for the dual variables with respect to the usual case: in place of relative number and phase among two macroscopic phase-coherent objects, we obtain here the Josephson oscillations of the average current and its conjugate phase on a ring. We refer to the following section for the detailed derivation.

Projected Gross-Pitaevskii equation To model the finite temperature weakly interacting regime $\gamma \ll 1$ we use the classical field methodology and more precisely the projected Gross-Pitaevskii equation (PGPE) [29, 30]:

$$i\hbar \frac{\partial \psi_C}{\partial t} = P_C \left[\left(-\frac{\hbar^2}{2m} \frac{\partial^2}{\partial x^2} + P_C [V(x) + g|\psi_C|^2] \right) \psi_C \right],$$

where ψ_C is the classical field, obtained by restricting the system to the highly populated modes only (which can be treated classically) and $P_C[\dots]$ is the projector onto this subspace. This projector is implemented in the single particle momentum basis, by defining a cutoff on the wavevectors k . We follow the rule $k_{\text{cut}} \leq 2k_{\text{grid}}/3$ to avoid aliasing and enforce momentum conservation (in the absence of the barrier), even in the presence of a non negligible thermal fraction [42]. To prepare the initial state we sample an equilibrium thermal state using a stochastic PGPE [43, 44] while fixing the average number of particles [45]. The simulation is ran typically 100 times with different initial states and measured quantities are

averaged over this ensemble. The PGPE is particularly relevant to model 1D Bose gases at finite temperature, in the quasi-condensate regime, allowing to perform quantitative comparison with experiments [30].

Tonks-Girardeau regime To describe the limit of strongly interacting bosons, $\gamma \gg 1$, we focus on the Tonks-Girardeau (TG) limit of infinitely strong repulsive interactions, and model the dynamics by using the exact TG solution [31]. In particular, we make use of the time-dependent Bose-Fermi mapping [31–33], where the many-body wavefunction Ψ_{TG} reads

$$\Psi_{TG}(x_1, \dots, x_N) = \prod_{1 \leq j < \ell \leq N} \text{sgn}(x_j - x_\ell) \det[\psi_k(x_j, t)], \quad (3)$$

where $\psi_j(x, t)$ is the single-particle solution of the Schrödinger equation $i\hbar \partial_t \psi_j = [-\hbar^2 \partial_x^2 / 2m + V(x, t)] \psi_j$ with initial conditions $\psi_j(x, 0) = \psi_j^0$, with ψ_j^0 being the eigenfunctions of the Schrödinger equation at initial time. This approach allows to describe by an exact solution the full dynamics after the quantum quench provided by the phase imprinting. In detail, we write the initial wavefunction as the groundstate of a ring potential in the presence of a barrier $\alpha \delta(x)$, constructed by the first N single-particle orbitals $\psi_j^0(x)$, which we then multiply by a phase profile that is induced by the phase imprinting, obtaining the initial wavefunction $\chi_j(x) = e^{2\pi i \ell x / L} \psi_j^0(x)$. The evolution is calculated by projecting such state with the eigenbasis of the unperturbed system $\psi_n(x, t) = \sum_j \langle \psi_j^0 | \chi_n \rangle \psi_j^0(x) e^{-i\epsilon_j t / \hbar}$ and where ϵ_n is the n th single-particle eigenenergy [46, 47]. The current within the TG regime, as being a local quantity, can be easily calculated using the occupations amplitudes of the single-particle eigenbasis, which in our case is found upon the projection over the initial state, as :

$$j(x, t) = \frac{\hbar}{m} \text{Im} \left[\sum_n^{\infty} f(\epsilon_n) \psi_n^*(x, t) \partial_x \psi_n(x, t) \right] \quad (4)$$

with $f(\epsilon_n)$ being the Fermi-Dirac distribution. In this work we focus in particular on the average current flow along the ring, given by $J = \int dx j(x, t) / (LN)$.

Comparing different barriers We note that, in the thin-barrier limit, corresponding to $\sigma \ll n^{-1}$ and $\sigma \ll \xi$, where $\xi = \sqrt{\hbar^2 / 2mg\eta}$ is the healing length, the Gaussian and the delta barriers have a comparable effect and the strength of the delta barrier potential can be related to the parameters of Gaussian barrier through $V(x) = \alpha_{\text{eff}} \delta(x)$ with $\alpha_{\text{eff}} = \sqrt{2\pi\sigma} V_0$. This is useful to compare for example the dynamics obtained with the analytical two-mode model (with a delta barrier) to a full numerical simulation of the Gross-Pitaevskii equation (with a thin Gaussian barrier).

Two-mode model

In this section we present the generalized version of the two-mode model [28]. This extension of the model also corresponds to a generalization of the two-mode approach presented in [48], where all overlapping modes were real functions.

We define the two-mode wavefunction as:

$$\Psi(x, t) = \phi_1(t)\varphi_1(x) + \phi_2(t)\varphi_2(x),$$

fulfilling the orthonormalization condition:

$$\int_0^L dx \varphi_i^* \varphi_j = \delta_{i,j},$$

and where $\varphi_{1/2}$ are the x -coordinate representation of the wavefunctions build as a linear combinations of the first and second excited states of the system as follows:

$$\varphi_1(x) = \frac{(i\psi_1(x) + \psi_2(x))}{\sqrt{2}}, \quad \varphi_2(x) = \frac{(i\psi_1(x) - \psi_2(x))}{\sqrt{2}}.$$

$$\begin{aligned} \dot{z} = & -2\sqrt{(1-z^2)} \operatorname{Im} [K e^{i\theta}] + (1-z^2) |U_{2211}| \sin(2\theta - \arg(U_{2211})) \\ & + \sqrt{(1-z^2)} (1+z) |U_{2111}| \sin(\theta - \arg(U_{2111})) + \sqrt{(1-z^2)} (1-z) |U_{2221}| \sin(\theta - \arg(U_{2221})) \end{aligned} \quad (5)$$

$$\begin{aligned} \dot{\theta} = & [E_1^0 - E_2^0 + (U_{1111} - U_{2222})/2 + Nz(U_{1111} + U_{2222})/2 - 2z\Re[U_{1212}]] - z|U_{1122}| \cos(2\theta + \arg(U_{1122})) \\ & + 2K \cos(\theta) \frac{z}{\sqrt{(1-z^2)}} + \sqrt{(1-z^2)} [(|U_{1121}| \cos(\theta + \arg(U_{1121})) - |U_{2122}| \cos(\theta + \arg(U_{2122}))) \\ & + \frac{z}{\sqrt{(1-z^2)}} [(z-1)|U_{1222}| \cos(\theta + \arg(U_{1222})) - (z+1)|U_{2111}| \cos(\theta + \arg(U_{2111})))] \end{aligned} \quad (6)$$

with z and θ corresponding to the relative population of the positive/negative angular momentum states and their relative phase respectively. This new phase-space representation is defined from the probability amplitudes $\phi_i = \sqrt{N_i(t)} e^{i\theta_i(t)}$ and the parameters of the model are given by:

$$\begin{aligned} U_{i,j,k,l} &= g_{1D} \int_0^L dx \varphi_i^* \varphi_j^* \varphi_k \varphi_l, \\ K &= - \int_0^L dx \left[\frac{\hbar^2}{2m} \varphi_1^* \partial_x^2 \varphi_2 + V(x) \varphi_1^* \varphi_2 \right], \\ E_i^0 &= \int_0^L dx \left[\frac{\hbar^2}{2m} \varphi_i^* \partial_x^2 \varphi_i + V(x) |\varphi_i|^2 \right]. \end{aligned}$$

Mode-mode excitations

Here we discuss in detail the specific procedure followed when calculating the excitations generated in

Note that $\phi_i(t)$ represent the probability amplitude of populating state φ_i , which is a state carrying one positive/negative unit of angular momentum. For our purposes we will form φ_i as a combination of the first and second excited states of the noninteracting system, ψ_i , (which can be calculated analytically). Nonetheless, one can always calculate the first and second excited states of the interacting system from the GPE and then calculate the tunneling and interacting parameters appearing in the model.

By introducing the previous ansatz into the GPE equation and integrating over the spatial coordinate one obtains two coupled equations that can be rewritten in the relative coordinates representation $z = (N_1(t) - N_2(t))/N$ and $\theta = \theta_2 - \theta_1$ as:

the system after the angular momentum quench in the strongly interacting limit. In particular, we recall that Eq. (3) shows the current after a phase imprinting has been performed onto the ground state of the ring in the presence of the barrier.

In order to address each particular excitation of the system and its role in the dynamics we first rewrite Eq. (3) in its full form:

$$J = \frac{\hbar}{Nm} \operatorname{Im} \left[\sum_k \sum_j A_{j,k} e^{-i(\epsilon_j - \epsilon_k)t/\hbar} \right], \quad (7)$$

where $\chi_n(x) = e^{-2\pi i l x/L} \psi_n(x)$ with ψ_n being the eigenfunctions of the Schrödinger equation at initial time before the phase imprinting, and the amplitude of the ex-

citations is

$$A_{j,k} = \frac{\hbar}{m} \text{Im} \left[\sum_n^\infty f(\epsilon_n) \langle \chi_n | \psi_k \rangle \right. \quad (8)$$

$$\left. \langle \psi_j | \chi_n \rangle \int_0^L \frac{dx}{L} \psi_k^*(x) \partial_x \psi_j(x) \right], \quad (9)$$

with frequency of oscillation given by $\omega_{j,k} = \frac{\epsilon_j - \epsilon_k}{\hbar}$.

The excitations present in the system (shown in Fig. 3(c) of the main text) are produced during the quench protocol. In particular, we use a phase imprinting procedure that produces a highly excited state with respect to the system at rest, as all the particles start moving along the ring, going from a state with zero current to a circulating one.

As discussed previously, in the TG regime bosons are mapped to noninteracting fermions. Consequently, in order to excite particles to a circulating state, the system produces an excited state, for each individual initial non-moving state in the initial Fermi sphere, formed by a superposition of doublet states with an energy splitting proportional to the gap opened by the barrier (other excited states are also populated for larger barrier with increasing probability as the barrier strength increases). Therefore, the excitations observed in our system go beyond the usual single-particle excitation studied through the dynamical structure factor as multiple single-particle hole excitations occur.

Indeed, we identified multiple single particle-hole ex-

citations created at the same time (see for instance the number of curves for a given value of λ_{TG} in Fig. 3(c)). As an example, we identify that the excitation with higher amplitude, Eq. (9), corresponds to the lowest energy single particle-hole excitation that can be created in our system, which in our particular case with an odd number of particles corresponds to a frequency of oscillation $\omega_{N+2,N+1}$. However, we observe that in fact, many excitations with lower associated energy are also excited. The existence of those excitations is possible because of the form of our state just after the quench, which consists in a superposition of excited states of the unperturbed system, and not of a completely filled Fermi sphere. Note also that for weak barriers all relevant frequencies, have a very similar frequency of oscillations, $\omega_{i,j} \approx \omega_{k,l} \forall i, j, k, l$, and thus, the envelope over the main oscillation has a very long period.

We can conclude that the effective damping observed in our system goes to zero in the limit of an infinitely small barrier and on the contrary, for large barrier strengths, many excitations with different associated frequencies are present in the system producing an effective damping as the one shown in this work (see for instance inset of Fig. 3(a) of the main text). Moreover, when temperature is present the coherent processes of each individual particle, labeled by n in Eq. (9), are mixed by the Fermi distribution $f(\epsilon_n)$, giving rise to, as is also known in previous works, incoherent phase slips.